ChemBioChem

Research Article
doi.org/10.1002/cbic.202300006

Chemistry Europe
European Chemical Societies Publishing

www.chembiochem.org

Nutlin-3a-aa: Improving the Bioactivity of a p53/MDM2 Interaction Inhibitor by Introducing a Solvent-Exposed Methylene Group

Florian Nietzold,[a] Stefan Rubner,[a] Beata Labuzek,[b] Przemysław Golik,[b] Ewa Surmiak,[b] Xabier del Corte,[b, c] Radoslaw Kitel,[b] Christoph Protzel,[a] Regina Reppich-Sacher,[d] Jan Stichel,[d] Katarzyna Magiera-Mularz,[b] Tad A. Holak,[b] and Thorsten Berg*[a]

Nutlin-3a is a reversible inhibitor of the p53/MDM2 interaction. We have synthesized the derivative Nutlin-3a-aa bearing an additional exocyclic methylene group in the piperazinone moiety. Nutlin-3a-aa is more active than Nutlin-3a against purified wild-type MDM2, and is more effective at increasing p53 levels and releasing transcription of p53 target genes from MDM2-induced repression. X-ray analysis of wild-type MDM2-bound Nutlin-3a-aa indicated that the orientation of its modified piperazinone ring was altered in comparison to the piperazinone ring of MDM2-bound Nutlin-3a, with the exocyclic methylene group of Nutlin-3a-aa pointing away from the protein surface. Our data point to the introduction of exocyclic methylene groups as a useful approach by which to tailor the conformation of bioactive molecules for improved biological activity.

Introduction

A common indicator for carcinogenesis is dysregulation of the primary tumor suppressor p53, the function of which is pivotal for preserving DNA integrity and hence defending cells from malignant transformation.[1] The p53 protein is mutated or deleted in approximately 50% of human tumors.[2] Another frequently observed mechanism of p53 inactivation is through overexpression of its negative regulator, the E3 ubiquitin ligase MDM2, which blocks p53 activity by three different mechanisms: by binding to its transactivation domain, by promoting its nuclear export, and by targeting p53 for proteasomal degradation.[3] Overexpression of MDM2 by gene amplification is detected in up to 20% of human cancers.[4] A powerful approach by which to liberate p53 from MDM2 and thus restore p53 function is by the inhibition of p53/MDM2 complex formation by small-molecule ligands.[5] The *cis*-imidazoline MDM2 Nutlin-3a (**1**, Figure 1A) was among the first potent small-molecule inhibitors of the p53/MDM2 interaction.[6]

We recently designed the hydrophobically tagged MDM2 ligand Nutlin-3a-HT (**2**, Figure 1B) by attaching the hydrophobic tag HyT13[7] to the piperazinone ring of Nutlin-3a (**1**).[8] Nutlin-3a-HT (**2**) was more potent in restoring p53 functions than Nutlin-3a (**1**), presumably as a result of inducing MDM2 degradation.[8] Using MDM2/p53/Nutlin-3a as a model system, we wondered whether an irreversibly binding hydrophobically

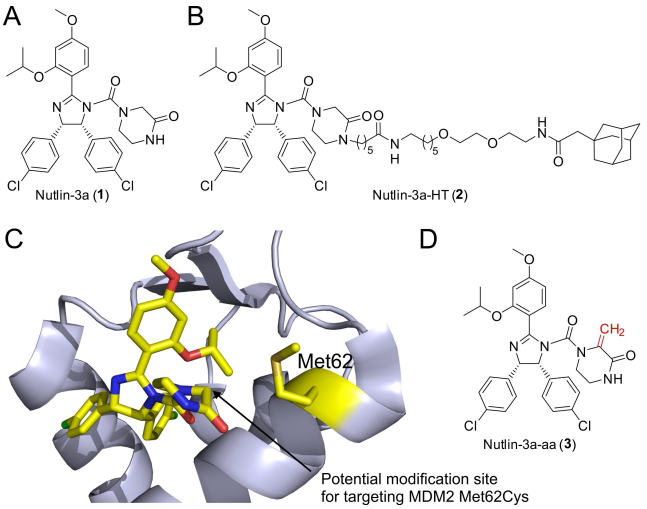

Figure 1. Structures of A) Nutlin-3a (**1**) and B) hydrophobically tagged Nutlin-3a-HT (**2**). C) X-ray structure of the Nutlin-3a/MDM2 complex (PBD ID: 4J3E).[9] The figure was generated by using PyMOL.[10] D) Structure of Nutlin-3a-aa (**3**).

[a] *Dr. F. Nietzold, Dr. S. Rubner, C. Protzel, Prof. Dr. T. Berg*
Institute of Organic Chemistry, Leipzig University
Johannisallee 29, 04103 Leipzig (Germany)
E-mail: tberg@uni-leipzig.de
[b] *Dr. B. Labuzek, Dr. P. Golik, Dr. E. Surmiak, X. del Corte, Dr. R. Kitel, Dr. K. Magiera-Mularz, Prof. Dr. T. A. Holak*
Department of Organic Chemistry, Faculty of Chemistry
Jagiellonian University
Gronostajowa 2, 30-387 Krakow (Poland)
[c] *X. del Corte*
Present address: Departamento de Química Orgánica I
Centro de Investigación y Estudios Avanzados "Lucio Lascaray"
Facultad de Farmacia, University of the Basque Country
UPV/EHU Paseo de la Universidad 7
01006 Vitoria-Gasteiz (Spain)
[d] *R. Reppich-Sacher, Dr. J. Stichel*
Institute of Biochemistry, Leipzig University
Brüderstraße 34, 04103 Leipzig (Germany)

Supporting information for this article is available on the WWW under https://doi.org/10.1002/cbic.202300006

tagged ligand would induce a substantially higher degree of protein degradation than the corresponding reversibly binding tagged inhibitor, given that the contact time with the target protein should be substantially increased. In a first step towards addressing this question, we aimed to design a protein-reactive Nutlin-3a derivative, with the intention of converting it to a hydrophobically tagged, irreversibly binding inhibitor in a second step. The crystal structure of Nutlin-3a (**1**) bound to humanized MDM2 from Xenopus[9] showed that one side of the piperazinone ring is in close proximity to the side chain of Met62 (Figure 1C); wild-type MDM2 does not carry a cysteine residue in its Nutlin-3a binding site. To create an irreversible protein-inhibitor pair, we exchanged MDM2 Met62 for cysteine, creating the point mutant protein MDM2 Met62Cys. We also designed Nutlin-3a-aa (**3**), bearing an acrylamide as a potential Michael acceptor (Figure 1D), by introducing an exocyclic methylene group into the piperazinone ring of Nutlin-3a (**1**). The cysteine side chain of MDM2 Met62Cys was intended to attack the acryl amide function of Nutlin-3a-aa (**3**) in a Michael addition.

Results and Discussion

To synthesize the modified piperazinone moiety bearing an exocyclic methylene group, racemic serine (**4**) was converted to the α-bromo-β-hydroxycarboxylic acid **5** by treatment with $NaNO_2$ and KBr in diluted H_2SO_4 (Figure 2A).[11] After conversion of the acid **5** to the ethyl ester **6**,[12] the hydroxy group was protected as a *tert*-butyldimethylsilylether to provide **7**. Reaction with 1,2-ethylenediamine, followed by ester cleavage, formed the piperazinone ring of **8** in a two-step procedure.[13] Amide bond formation between the silyl-protected **8** and the building block **9**, which had been prepared in diastereomerically pure form and an enantiomeric excess (*ee*) of 99% in a nine-step procedure[8] based on the synthetic methodology of Johnston,[14] provided **10** (Figure 2B). Treatment with an excess of Hendrickson reagent (triphenylphosphonium anhydride trifluoromethane sulfonate)[15] formed from 4 equivalents of Ph_3PO and 2 equivalents of Tf_2O, not only provided the desired imidazoline ring,[14] but also generated the exocyclic methylene group of **3** in one synthetic step.

Covalent modification of the MDM2 Met62Cys mutant by Michael addition of the cysteine's thiol side to the acrylamide moiety of **3** should result in a time-dependent increase in inhibitory activity. However, analysis of the ability of **3** to inhibit peptide binding to MDM2 Met62Cys in fluorescence polarization (FP) assays did not show time dependence over a period of up to 8 hours (Figure 3A). Consistently, mass spectrometric analysis of MDM2 Met62Cys after incubation with **3** did not provide evidence for covalent protein modification (Figure S1 in the Supporting Information). Nevertheless, **3** was slightly more potent than **1** against MDM2 Met62Cys in FP assays (**3**: $IC_{50} = 0.56 \pm 0.06$ μM; **1**: $IC_{50} = 0.87 \pm 0.18$ μM, Figure 3B).

Given that the steric demands of the amino acid at position 62 are higher in the wild-type protein (Met62) than in the Met62Cys mutant, we wondered whether the newly introduced

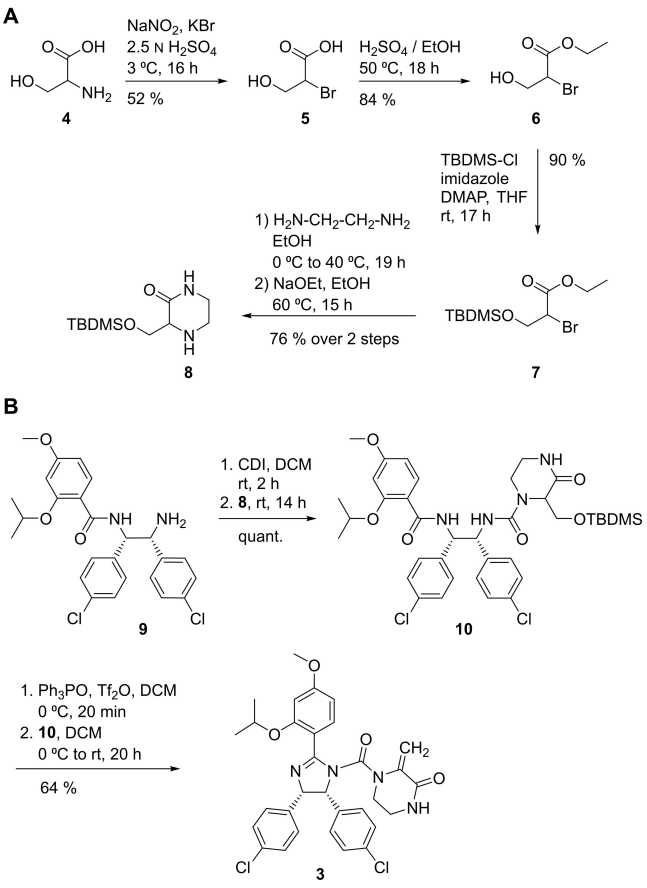

Figure 2. A) Synthesis of the piperazinone building block **8** and B) its conversion to Nutlin-3a-aa (**3**).

acrylamide moiety in Nutlin-3a-aa (**3**) would be tolerated by wild-type MDM2. Surprisingly, **3** inhibited wild-type MDM2 in FP assays with a twofold higher potency ($IC_{50} = 0.21 \pm 0.02$ μM, Figure 3C) than Nutlin-3a (**1**, $IC_{50} = 0.44 \pm 0.03$ μM). The activity of **3** against wild-type MDM2 was not time-dependent (Figure S2).

Binding of **3** to wild-type MDM2 was validated using $^{1}H,^{15}N$ HSQC NMR titration.[16] The method is based on the monitoring of chemical shift changes in protein amide backbone resonances upon protein titration with a small molecule. **3** displays a tight interaction with MDM2 (slow chemical exchange) which is indicated by the doubling of several peaks on the spectra of MDM2 protein titrated with 25% of the ligand (Figure S3). Such characteristics are specific for ligands with a dissociation constant (K_D) lower then approximately 1 μM, which is also the methodology limit.[17] The chemical shift changes pattern for compound **3** is similar to the typical interaction between small molecules and MDM2, and its analysis indicated that the ligand is placed in the binding pocket of the MDM2 protein.[18]

In order to understand the increased activity of **3** against wild-type MDM2 as compared to Nutlin-3a (**1**), we co-crystallized **3** with human MDM2 and solved the X-ray structure of the complex (Figures 4 and S4, Table S1). In comparison with the structure of MDM2-bound **1** (PDB ID: 4J3E),[9] the orientation of

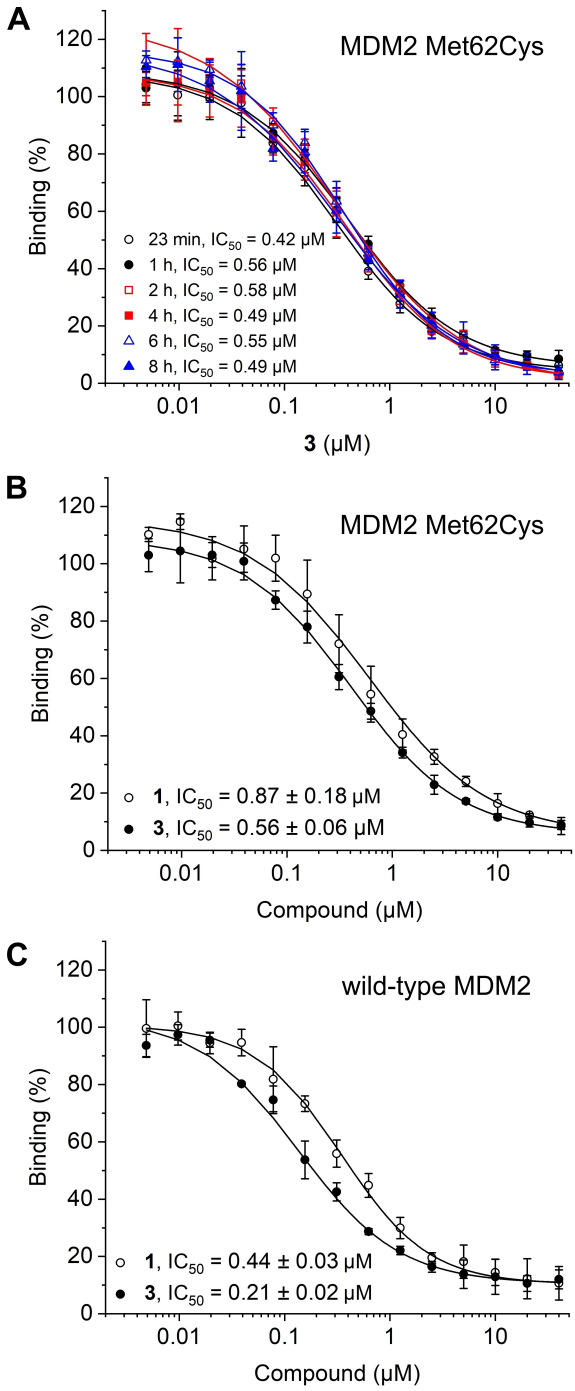

Figure 3. A) Analysis of the time-dependent activity of Nutlin-3a-aa (**3**) against MDM2 Met62Cys in FP assays. Activities of **1** and **3** against B) MDM2 Met62Cys and C) wild-type MDM2 in FP assays. Error bars represent standard deviations ($n = 3$).

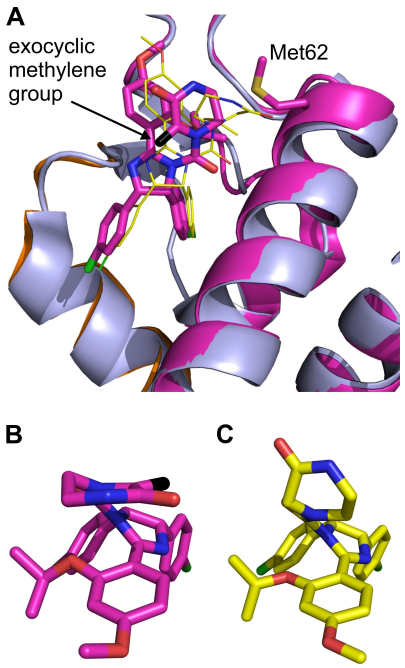

Figure 4. A) Overlay of the X-ray structure of **3** (shown with its exocyclic methylene carbon atom in black, the other carbon atoms in magenta) in complex with human MDM2 (protein shown in magenta and orange) and the published X-ray structure of Nutlin-3a (**1**) in complex with humanized MDM2 from Xenopus (**1** shown with carbon atoms in yellow, protein shown in lilac, PBD ID: 4J3E).[9] Amino acids of human MDM2 shown in orange are derived from an adjacent protein molecule. See Figure S4 for the complete structure. Conformations of B) **3** and C) **1** in the MDM2-bound states as shown in (A). The figure was generated using PyMOL.[10]

the piperazinone ring of **3** in complex with human wild-type MDM2 was found to be reversed. In consequence, the exocyclic methylene group of **3** is orientated away from MDM2 Met62 (Figure 4A). The introduction of the exocyclic methylene group also induces a more planar conformation of the piperazinone ring in **3** (Figure 4B), as compared to the piperazinone ring of **1** (Figure 4C). The conformation of **3** in the MDM2-bound state suggests that the imidazoline-bisalkoxyphenyl unit might engage in stabilizing intramolecular interactions with the acrylamide moiety (Figure 4B). A piperazinone ring orientation similar to that observed in complex with wild-type MDM2 might explain the observed lack of covalent inhibition of MDM2 Met62Cys by **3**. A crystal structure of MDM2 Met62Cys in complex with **3** would be required to confirm whether this is the case. While numerous acrylamides are known to be cysteine-reactive protein inhibitors,[19] we cannot rule out the possibility that the lack of detected reactivity between **3** and MDM2 Met62Cys is caused by either a reduced Michael acceptor reactivity of **3** owing to the adjacent ureido motif, or insufficient deprotonation of the MDM2 Cys62 thiol side chain to the more nucleophilic thiolate.

An interesting feature of the X-ray structure is that the α-helix comprising amino acids Glu95-Asn106, which provides the hydrophobic pocket for one of the chlorophenyl rings of **3**, is provided by an adjacent protein molecule in the crystal. Each molecule **3** is therefore bound to two separate protein molecules (Figure S4). We believe that this arrangement of protein units is not relevant in solution. According to one-dimensional spectra, the line-width of the aliphatic peaks of MDM2 in the presence of **3** shows a slight broadening of the peaks compared to the reference apo-MDM2, which may indicate some form of oligomerization or aggregation of the protein in the presence of the ligand (Figure S5). Nevertheless,

this change is not substantial and is much smaller than in the presence of a compound previously shown to induce dimerization of MDM2 in solution.[20] Analytical gel filtration of MDM2 in the presence or absence of **3** did not shift the MDM2 elution peak (Figure S6), confirming that protein dimerization as observed in the X-ray structure (Figures 4 and S4) is likely to be a crystallization artifact.

Transcriptional activation of MDM2 by p53 is part of the negative feedback loop which tightly regulates p53 activity in the absence of cellular stress. Another target activated by p53 is the cell cycle suppressor p21. Treatment of human colon carcinoma cells (HCT-116) with Nutlin-3a (**1**) induced a dose-dependent increase in p53 and, in consequence, its transcriptional targets MDM2 and p21, as previously reported in the literature (Figure 5A, B).[6] In parallel experiments, cells treated with **3** showed an approximately 2-fold higher protein concentration of p53 (Figure 5A, B), as well as significantly higher concentrations of MDM2 (Figure 5A, C) and p21 (Figure 5A, D), than cells treated with **1** at the corresponding molar concentrations. This demonstrates that the higher activity of **3** as compared to **1** against wild-type MDM2 seen in FP assays (Figure 3C) is also observed in cultured human tumor cells.

Conclusion

In summary, we have synthesized Nutlin-3a-aa (**3**), based on the reversible MDM2 inhibitor Nutlin-3a (**1**), with the intention of creating an irreversible inhibitor of the MDM2 point mutant Met62Cys. While **3** exhibited higher potency than **1** against MDM2 Met62Cys, it did not act as an irreversible inhibitor, as supported by the absence of time-dependent inhibition and the lack of detected covalent protein modification of MDM2 Met62Cys. Nevertheless, **3** displayed superior activity to **1** against wild-type MDM2 in biochemical assays and in cultured human tumor cells. Crystallographic analysis demonstrated that the exocyclic methylene group of **3** is not engaged in protein contacts with wild-type MDM2. Instead, it induces a more planar conformation of the piperazinone ring and a reversal of its orientation, resulting in the exocyclic methylene group facing away from the protein. This observation was particularly unexpected because of the lipophilicity of the methylene group. The installation of methyl groups is a well-established approach by which to achieve conformational preorganization of organic molecules, including those with aliphatic rings systems.[21] In contrast, the introduction of exocyclic methylene groups on aliphatic ring systems to affect the conformations of reversibly binding inhibitors is less common in medicinal chemistry, despite some reports on nucleoside analogs[22] and potent natural product derivatives[23] containing this functional group. The introduction of exocyclic methylene groups could therefore represent a promising approach by which to tailor the conformation of bioactive molecules for improved biological activity.

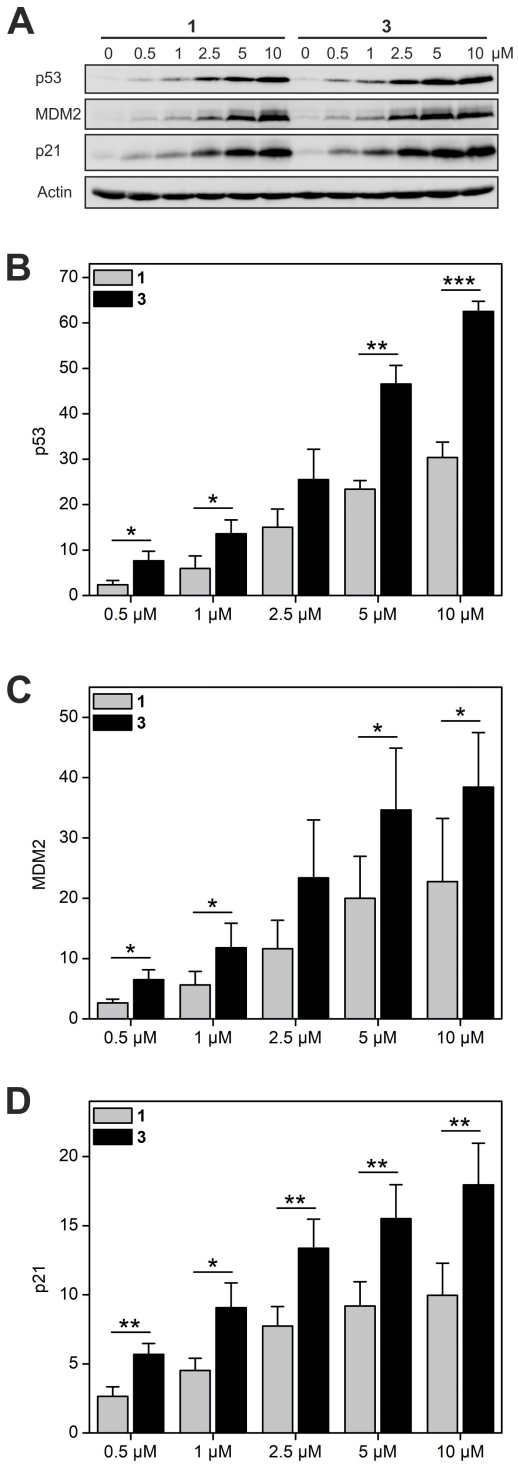

Figure 5. A) Effect of Nutlin-3a (**1**) and Nutlin-3a-aa (**3**) on the protein levels of p53, MDM2, and p21 in HCT-116 cells ($n = 3$). Fold increase in protein levels of B) p53, C) MDM2, and D) p21 in cells treated with **1** and **3** as compared to DMSO-treated cells. A Student's t-test was carried out for the comparison of protein concentrations in the presence of **1** and **3**. * $p < 0.05$; ** $p < 0.01$; *** $p < 0.001$ (t-test, two-tailed, paired).

Experimental Section

Fluorescence polarization assays: Fluorescence polarization assays were essentially carried out as previously described.[8] Nutlin-3a (**1**)

and Nutlin-3a-aa (**3**) were tested for their abilities to interfere with binding between the p53-derived peptide 5-carboxyfluorescein-RFMDYWEGL-OH and MDM2 (amino acids 1–119), ether wild-type or the Met62Cys mutant. The final concentration of buffer components used was 10 mM Tris, 50 mM NaCl, 1 mM EDTA, 0.1% NP-40 substitute, 1 mM TCEP, and 2% DMSO, titrated to pH 8.0. Dilution series of test compounds in buffer were incubated with the protein (final concentrations: 27 nM for wild-type MDM2, 24 nM for MDM2 Met62Cys) for 1 h at room temperature, followed by addition of the fluorescent-labeled peptide (final concentration: 10 nM). Unless stated otherwise, fluorescence polarization was measured 1 h after addition of the fluorescent-labeled peptide using a Tecan Infinite F500 microplate reader (λ_{ex} = 485 nm, λ_{em} = 535 nm). Data were analyzed using OriginPro 2019 software. Fluorescence polarization values were converted to % inhibition via the binding curve between fluorescent peptide and protein. Compound concentrations at which 50% inhibition of protein binding activity was observed are given as IC_{50} values. Conversion of IC_{50} values to K_i values was carried out using the published equation (K_d values: wild-type MDM2: 26 nM; MDM2 Met62Cys mutant: 20 nM).[24]

Protein crystallization: Co-crystallization of human MDM2 (residues 18–125) with Nutlin-3a-aa was performed using the standard sitting drop vapor diffusion method at 4 °C. Briefly, 1 μL drops of protein-inhibitor solution in a molar ratio of 1:3 were mixed with equal volumes of the reservoir solution containing 0.01 M magnesium chloride hexahydrate, 0.05 M Tris hydrochloride pH 7.6, 1.6 M ammonium sulfate, and were allowed to equilibrate against the reservoir. Co-crystals of the human MDM2-Nutlin-3a-aa complex appeared after 24 h. The crystals were flash-cooled in liquid nitrogen using 25% glycerol in mother liquor for cryo-protection.

Data collection and structure solution: X-ray diffraction data was collected at beamline MX 14.1 at Helmholtz-Zentrum Berlin, Germany. The data was indexed and integrated with XDSAPP and scaled with Aimless.[25] The initial phases were obtained by molecular replacement using Phaser[26] and MDM2 search model derived from PDB ID: 4ZFI. The model was built in the resulting electron density using COOT[27] and omit map strategy, followed by refinement with Refmac 5.[28] R_{free} was selected to monitor the structure refinement strategy.[29] The statistics of data collection and refinement are summarized in Table S1.

Western blot: Experiments were carried out essentially as described.[8] Cell lysates containing a total protein amount of 40 μg were separated by SDS-PAGE on a 10% polyacrylamide gel and transferred to a nitrocellulose membrane. Cellular levels of MDM2, p53, and p21 were analyzed using rabbit monoclonal antibodies against p53, MDM2, and p21 (1:1000, Cell Signaling), and reblotted with β-actin (1:1000, Cell Signaling). Membranes were incubated with secondary antibody swine anti-rabbit HRP (1:3000, Dako). ECL was performed using Western Lightning Plus chemiluminescence reagent (Perkin-Elmer). After visualization using an ImageQuant digital imaging system (GE Healthcare), quantitation was carried out using ImageJ software (NIH).[30] Experiments were performed in triplicate.

Acknowledgements

This work was generously supported by the Deutsche Forschungsgemeinschaft (BE 4572/3-1 to T.B.). We extend our thanks to Barbara Klüver, Katrin Eckhardt, Nadiya Brovchenko, and Domenique Herbstritt for experimental support. Parts of the data described in this manuscript have been published in the dissertation of Florian Nietzold (Leipzig University, 2019).[31] *In addition, this work was financially supported by the National Science Centre, Poland (NCN) under Grant Symphony 2014/12/W/NZ1/00457 (to T.A.H). We thank HZB for the allocation of synchrotron radiation beamtime. We acknowledge the MCB Structural Biology Core Facility (supported by the TEAM TECH CORE FACILITY/2017-4/6 grant from the Foundation for Polish Science) for valuable support. Open Access funding enabled and organized by Projekt DEAL.*

Conflict of Interest

The authors declare no conflict of interest.

Data Availability Statement

The data that support the findings of this study are available in the supplementary material of this article. Coordinates for **3** bound to MDM2 have been deposited in the Protein Data Bank under accession code 8AEU.

Keywords: biological activity · drug design · inhibitors · protein structures · protein-protein interactions

[1] a) D. P. Lane, *Nature* **1992**, *358*, 15–16; b) S. Prost, C. O. C. Bellamy, A. R. Clarke, A. H. Wyllie, D. J. Harrison, *FEBS Lett.* **1998**, *425*, 499–504.
[2] D. Hamroun, S. Kato, C. Ishioka, M. Claustres, C. Beroud, T. Soussi, *Hum. Mutat.* **2006**, *27*, 14–20.
[3] D. A. Freedman, L. Wu, A. J. Levine, *Cell. Mol. Life Sci.* **1999**, *55*, 96–107.
[4] J. Momand, D. Jung, S. Wilczynski, J. Niland, *Nucleic Acids Res.* **1998**, *26*, 3453–3459.
[5] N. Estrada-Ortiz, C. G. Neochoritis, A. Dömling, *ChemMedChem* **2016**, *11*, 757–772.
[6] L. T. Vassilev, B. T. Vu, B. Graves, D. Carvajal, F. Podlaski, Z. Filipovic, N. Kong, U. Kammlott, C. Lukacs, C. Klein, N. Fotouhi, E. A. Liu, *Science* **2004**, *303*, 844–848.
[7] T. K. Neklesa, H. S. Tae, A. R. Schneekloth, M. J. Stulberg, T. W. Corson, T. B. Sundberg, K. Raina, S. A. Holley, C. M. Crews, *Nat. Chem. Biol.* **2011**, *7*, 538–543.
[8] F. Nietzold, S. Rubner, T. Berg, *Chem. Commun.* **2019**, *55*, 14351–14354.
[9] B. Vu, P. Wovkulich, G. Pizzolato, A. Lovey, Q. Ding, N. Jiang, J. J. Liu, C. Zhao, K. Glenn, Y. Wen, C. Tovar, K. Packman, L. Vassilev, B. Graves, *ACS Med. Chem. Lett.* **2013**, *4*, 466–469.
[10] *The PyMOL Molecular Graphics System*, Version 0.99 Schrödinger, LLC.
[11] A. R. Glabe, K. L. Sturgeon, S. B. Ghizzoni, W. K. Musker, J. N. Takahashi, *J. Org. Chem.* **1996**, *61*, 7212–7216.
[12] F. Wojciechowski, R. H. E. Hudson, *Nucleosides Nucleotides Nucleic Acids* **2007**, *26*, 1195–1198.
[13] A. Benjahad, R. Benhaddou, R. Granet, M. Kaouadji, P. Krausz, S. Piekarski, F. Thomasson, C. Bosgiraud, S. Delebassée, *Tetrahedron Lett.* **1994**, *35*, 9545–9548.
[14] T. A. Davis, A. E. Vilgelm, A. Richmond, J. N. Johnston, *J. Org. Chem.* **2013**, *78*, 10605–10616.
[15] a) J. B. Hendrickson, M. S. Hussoin, *J. Org. Chem.* **1987**, *52*, 4137–4139; b) J. B. Hendrickson, M. S. Hussoin, *J. Org. Chem.* **1989**, *54*, 1144–1149.
[16] a) E. Barile, M. Pellecchia, *Chem. Rev.* **2014**, *114*, 4749–4763; b) R. Powers, *Expert Opin. Drug Discovery* **2009**, *4*, 1077–1098; c) S. B. Shuker, P. J. Hajduk, R. P. Meadows, S. W. Fesik, *Science* **1996**, *274*, 1531–1534.
[17] a) L. Fielding, *Prog. Nucl. Magn. Reson. Spectrosc.* **2007**, *51*, 219–242; b) M. P. Williamson, *Prog. Nucl. Magn. Reson. Spectrosc.* **2013**, *73*, 1–16.
[18] R. Stoll, C. Renner, S. Hansen, S. Palme, C. Klein, A. Belling, W. Zeslawski, M. Kamionka, T. Rehm, P. Mühlhahn, R. Schumacher, F. Hesse, B. Kaluza, W. Voelter, R. A. Engh, T. A. Holak, *Biochemistry* **2001**, *40*, 336–344.

[19] R. Roskoski, *Pharmacol. Res.* **2021**, *165*, 105422.
[20] E. Surmiak, A. Twarda-Clapa, K. M. Zak, B. Musielak, M. D. Tomala, K. Kubica, P. Grudnik, M. Madej, M. Jablonski, J. Potempa, J. Kalinowska-Tluscik, A. Dömling, G. Dubin, T. A. Holak, *ACS Chem. Biol.* **2016**, *11*, 3310–3318.
[21] a) H. Schönherr, T. Cernak, *Angew. Chem. Int. Ed.* **2013**, *52*, 12256–12267; *Angew. Chem.* **2013**, *125*, 12480–12492; b) E. J. Barreiro, A. E. Kümmerle, C. A. M. Fraga, *Chem. Rev.* **2011**, *111*, 5215–5246; c) C. S. Leung, S. S. F. Leung, J. Tirado-Rives, W. L. Jorgensen, *J. Med. Chem.* **2012**, *55*, 4489–4500.
[22] a) P. P. Seth, C. R. Allerson, A. Berdeja, A. Siwkowski, P. S. Pallan, H. Gaus, T. P. Prakash, A. T. Watt, M. Egli, E. E. Swayze, *J. Am. Chem. Soc.* **2010**, *132*, 14942–14950; b) P. Gunaga, M. Baba, L. S. Jeong, *J. Org. Chem.* **2004**, *69*, 3208–3211.
[23] a) P. Heretsch, A. Büttner, L. Tzagkaroulaki, S. Zahn, B. Kirchner, A. Giannis, *Chem. Commun.* **2011**, *47*, 7362–7364; b) J. Moschner, A. Chentsova, N. Eilert, I. Rovardi, P. Heretsch, A. Giannis, *Beilstein J. Org. Chem.* **2013**, *9*, 2328–2335.
[24] Z. Nikolovska-Coleska, R. Wang, X. Fang, H. Pan, Y. Tomita, P. Li, P. P. Roller, K. Krajewski, N. G. Saito, J. A. Stuckey, S. Wang, *Anal. Biochem.* **2004**, *332*, 261–273.
[25] P. R. Evans, G. N. Murshudov, *Acta Crystallogr. D Biol. Crystallogr.* **2013**, *69*, 1204–1214.
[26] A. J. McCoy, R. W. Grosse-Kunstleve, P. D. Adams, M. D. Winn, L. C. Storoni, R. J. Read, *J. Appl. Crystallogr.* **2007**, *40*, 658–674.
[27] P. Emsley, B. Lohkamp, W. G. Scott, K. Cowtan, *Acta Crystallogr. D Biol. Crystallogr.* **2010**, *66*, 486–501.
[28] G. N. Murshudov, P. Skubák, A. A. Lebedev, N. S. Pannu, R. A. Steiner, R. A. Nicholls, M. D. Winn, F. Long, A. A. Vagin, *Acta Crystallogr. D Biol. Crystallogr.* **2011**, *67*, 355–367.
[29] A. T. Brünger, *Nature* **1992**, *355*, 472–475.
[30] C. A. Schneider, W. S. Rasband, K. W. Eliceiri, *Nat. Methods* **2012**, *9*, 671–675.
[31] F. Nietzold, *Dissertation*, Leipzig University (Germany), **2019**.

Manuscript received: January 4, 2023
Accepted manuscript online: January 5, 2023
Version of record online: February 16, 2023